

FIG. 1. Feynman diagram for the process

$$\begin{array}{l} \nu N \rightarrow L^- + \text{anything} \\ \nu + L^- \rightarrow \bar{\nu}_1 \end{array}$$

The intermediate line is taken to be the mass shell. k and p are momenta of the incident ν and N , respectively, k' is the momentum of the heavy lepton L^- , K is the momentum of the final ν which is associated with the leptonic current for L , and Q and \bar{k} are the momenta of L^- and $\bar{\nu}_1$, respectively.

The corresponding expressions for incident $\bar{\nu}$ or μ^+ producing charged and neutral heavy leptons can be trivially obtained from expressions for reaction (2).

A. The production process

The amplitude $A_{\lambda\lambda'}$ for the production of a heavy lepton of helicity λ' from an incident neutrino of helicity λ can be expressed as⁸

$$\begin{aligned} \vec{B}_0 = & -\frac{2hG_1^2 m_L}{8\pi^2 k \cdot p} \left[\vec{k} \left(2W_1 + \frac{W_2}{M^2} p^2 + \frac{W_4}{M^2} q^2 + \frac{W_5}{M^2} q \cdot p \right) + \vec{p} \left(-2\frac{W_2}{M^2} k \cdot p - \frac{1+h^2}{2h} \frac{W_3}{M^2} q \cdot k - \frac{W_5}{M^2} q \cdot k \right) \right. \\ & \left. + \vec{q} \left(\frac{1+h^2}{2h} \frac{W_3}{M^2} k \cdot p - 2\frac{W_4}{M^2} k \cdot q - \frac{W_5}{M^2} k \cdot p \right) \right] \end{aligned} \quad (8)$$

and

$$\begin{aligned} A_0 = & -\frac{G_1^2(1+h^2)m_L}{8\pi^2 k \cdot p} \left[2k_0 W_1 + \frac{W_2}{M^2} (k_0 p^2 - 2p_0 k \cdot p) - \frac{W_3}{M^2} \frac{2h}{1+h^2} (p_0 k \cdot q - q_0 k \cdot p) + \frac{W_4}{M^2} (q^2 k_0 - 2q_0 k \cdot q) \right. \\ & \left. + \frac{W_5}{M^2} (k_0 p \cdot q - p_0 q \cdot k - q_0 k \cdot p) \right], \end{aligned} \quad (9)$$

where k_0 , q_0 , and p_0 are the zeroth components of k , q , and p , and m_L is the mass of heavy lepton L .

$$A_{\lambda\lambda'} = \frac{G_1}{\sqrt{2}} \bar{U}_L(k', \lambda') J(1+h\gamma_5) U_\nu(k, \lambda), \quad (5)$$

where J is the hadronic current, G_1 is the analog of the Fermi constant for the coupling of the heavy lepton to the nucleon at the production vertex (see Fig. 1), and $h = \pm 1$ if the heavy lepton couples via $(V \mp A)$, respectively. We describe the hadronic vertex of the reaction in terms of the structure functions defined by⁴

$$\begin{aligned} W_{\mu\nu} = & -\delta_{\mu\nu} W_1 - \frac{1}{M^2} p_\mu p_\nu W_2 - \frac{1}{2M^2} \epsilon_{\mu\nu\alpha\beta} p_\alpha q_\beta W_3 \\ & - \frac{1}{M^2} q_\mu q_\nu W_4 - \frac{1}{2M^2} (p_\mu q_\nu + p_\nu q_\mu) W_5, \end{aligned} \quad (6)$$

where M is the mass of the target nucleon, and $q = k - k'$, the momentum transfer from the leptons to the hadrons. The state of the produced lepton L in its rest frame can then be described by a (2×2) density matrix of the form

$$\rho_0 = \frac{1}{2} \left(1 + \vec{\sigma} \cdot \frac{\vec{B}_0}{A_0} \right), \quad (7)$$

where the σ 's are 2×2 Pauli matrices, and the vector \vec{B}_0/A_0 gives the polarization of L in its rest frame. In this frame, where $\vec{k}' = \vec{k} - \vec{q} = 0$, \vec{B}_0 is expressed, for convenience in subsequent generalization to a covariant frame, in terms of the dependent three-vectors, \vec{k} , \vec{q} , and \vec{p} as

The cross section for production of heavy leptons is directly related to the function A_0 and is given in the lab frame by

$$\begin{aligned} \frac{d\sigma_p}{dq^2 d\nu} = & -\frac{G_1^2(1+h^2)}{8ME^2\pi} \left[2k' \cdot kW_1 + \frac{W_2}{M^2} (k' \cdot k p^2 - 2k' \cdot p k \cdot p) + \frac{2h}{1+h^2} \frac{W_3}{M^2} (k' \cdot q k \cdot p - k' \cdot p k \cdot q) + \frac{W_4}{M^2} (k' \cdot k q^2 - 2k' \cdot q k \cdot q) \right. \\ & \left. + \frac{W_5}{M^2} (k' \cdot k p \cdot q - k' \cdot p k \cdot q - k' \cdot q k \cdot p) \right], \end{aligned} \quad (10)$$

where E is the incident lepton energy in the lab frame, and $\nu = -q \cdot p/M$.

B. Decay of the heavy lepton

The amplitude for the decay of a heavy lepton L of helicity λ' to a ν of helicity λ_f via a reaction of the type

$$L^-(k', \lambda') \rightarrow \nu(K, \lambda_f) + l^-(Q) + \bar{\nu}_i(\bar{k})$$

is expressed as

$$d_{\lambda' \lambda_f} = \frac{G_2}{\sqrt{2}} [\bar{U}_\nu(K, \lambda_f) \gamma_\mu (1 + g \gamma_5) U_L(k', \lambda')] \times [\bar{U}_i(Q) \gamma_\mu (1 + \gamma_5) V_{\nu_i}(\bar{k})], \quad (11)$$

where again $g = \pm 1$ depending on whether L couples via $(V \mp A)$, respectively.⁹

In the rest frame of the heavy lepton, the decay matrix for the process can be written as

$$\mathfrak{D}_0 = \gamma_0 \left[1 + \vec{\sigma} \cdot \frac{\vec{\beta}_0}{\gamma_0} \right], \quad (12)$$

where

$$\gamma_0 = -32G_2^2 m_L [(1 + g)^2 \bar{k}_0 K \cdot Q + (1 - g)^2 Q_0 K \cdot \bar{k}] \quad (13)$$

and

$$\vec{\beta}_0 = -32G_2^2 m_L [(1 + g)^2 \vec{k} K \cdot Q + (1 - g)^2 \vec{Q} K \cdot \bar{k}]. \quad (14)$$

The rate for the decay of a polarized heavy lepton to leptons is then given by

$$\Gamma_{L \rightarrow i} = \frac{1}{(2\pi)^5} \frac{1}{2m_L} \int \frac{d^3Q}{2Q_0} \frac{d^3K}{2K_0} \frac{d^3\bar{k}}{2\bar{k}_0} \times \delta^4(k' - K - Q - \bar{k})^{\frac{1}{2}} \text{Tr}(\rho \mathfrak{D}_0), \quad (15)$$

where ρ is any density matrix specifying the polarization state of the heavy lepton.

C. Production and subsequent decay of the heavy lepton

Taking the trace of the matrix $(\rho_0 \mathfrak{D}_0)$ and generalizing to a covariant form we get the required expression for the cross section for process of Fig. 1 as

$$\sigma = \frac{G_1^2 G_2^2}{8(2\pi)^7 [(k \cdot p)^2 - m_i^2 \cdot M^2]^{1/2} m_L \Gamma} I, \quad (16)$$

where

$$I = \int \frac{d^3k'}{2k'_0} \frac{d^3Q}{2Q_0} \frac{d^3\bar{k}}{2\bar{k}_0} \frac{d^3K}{2K_0} \delta^4(k' - \bar{k} - K - Q) T, \quad (17)$$

m_i is the mass of the incident lepton, Γ is the total width¹⁰ of L , and

$$T = 64(1 + g)^2 K \cdot Q \left\{ 2W_1 [2hm_L^2 k \cdot \bar{k} + (1 + h)^2 k' \cdot k k' \cdot \bar{k}] + \frac{W_2}{M^2} [2hm_L^2 (p^2 k \cdot \bar{k} - 2k \cdot p \bar{k} \cdot p) + (1 + h)^2 k' \cdot \bar{k} (k' \cdot k p^2 - 2k' \cdot p k \cdot p)] \right. \\ - \frac{W_3}{M^2} [(1 + h)^2 k' \cdot \bar{k} (k' \cdot p k \cdot q - k' \cdot q k \cdot p) + (1 + h^2) m_L^2 (k \cdot q \bar{k} \cdot p - k \cdot p \bar{k} \cdot q)] \\ + \frac{W_4}{M^2} [2hm_L^2 (q^2 k \cdot \bar{k} - 2k \cdot q \bar{k} \cdot q) + (1 + h)^2 k' \cdot \bar{k} (k' \cdot k q^2 - 2k' \cdot q k \cdot q)] \\ \left. + \frac{W_5}{M^2} [2hm_L^2 (q \cdot p k \cdot \bar{k} - q \cdot k p \cdot \bar{k} - q \cdot \bar{k} k \cdot p) + (1 + h)^2 k' \cdot \bar{k} (k' \cdot k p \cdot q - k' \cdot p k \cdot q - k' \cdot q k \cdot p)] \right\} \\ + 64(1 - g)^2 K \cdot \bar{k} \left\{ 2W_1 [-2hm_L^2 k \cdot Q + (1 - h)^2 k' \cdot k k' \cdot Q] \right. \\ + \frac{W_2}{M^2} [-2hm_L^2 (p^2 k \cdot Q - 2k \cdot p p \cdot Q) + (1 - h)^2 k' \cdot Q (k' \cdot k p^2 - 2k' \cdot p k \cdot p)] \\ - \frac{W_3}{M^2} [(1 - h)^2 k' \cdot Q (k' \cdot q k \cdot p - k' \cdot p k \cdot q) + (1 + h^2) m_L^2 (k \cdot p q \cdot Q - k \cdot q p \cdot Q)] \\ + \frac{W_4}{M^2} [-2hm_L^2 (q^2 k \cdot Q - 2k \cdot q q \cdot Q) + (1 - h)^2 k' \cdot Q (q^2 k' \cdot k - 2k' \cdot q k \cdot q)] \\ \left. + \frac{W_5}{M^2} [-2hm_L^2 (q \cdot p Q \cdot k - k \cdot p q \cdot Q - k \cdot q p \cdot Q) + (1 - h)^2 k' \cdot Q (k' \cdot k q \cdot p - k' \cdot p k \cdot q - k' \cdot q k \cdot p)] \right\}. \quad (18)$$

It may be worth mentioning that expressions (16) to (18), for the cross section for production and decay of charged heavy leptons L^\pm via reactions of the type (2), are exact. However, for the production and decay of neutral heavy leptons, L^0 or \bar{L}^0 , via reactions of types (3) and (4), the expressions for the cross section obtained above is correct only to the extent that the incident lepton mass $m_l = 0$.

D. Phase-space integration and the differential cross section

Neglecting the electron and muon mass the phase-space integration, over the unobserved pair of leptons in the decay products, is carried out analytically yielding I of the general form

$$I = \int \frac{d^3k'}{2k'_0} \frac{d^3Q}{2Q_0} F(k' \cdot Q) \theta(-(k' - Q)^2), \quad (19)$$

where F is a quadratic function of $(k' \cdot Q)$ and is given in the Appendix. We next introduce a coordinate system in the lab frame, shown in Fig. 2, in which the incident lepton beam with three-momenta \vec{k} is along the Z axis, \vec{k}' the three-momentum of the produced heavy lepton lies in the ZX plane, making an angle θ' with the Z axis, and θ and ϕ are the polar and azimuthal angles of \vec{Q} , the three-momentum of the charged lepton which is under observation. Since I , in Eq. (19), is quadratic in $\cos\phi$, the integration over ϕ can be done trivially to yield

$$\begin{aligned} \frac{d\sigma}{dq^2 dv dQ_t^2 dQ_l} &= \frac{G_1^2 G_2^2}{48(2\pi)^5 m_L \Gamma M E^2 Q_0} \\ &\times [(A_{0Q} + \frac{1}{2}A_{2Q})\Phi_Q + A_{1Q} \sin\Phi_Q \\ &+ \frac{1}{4}A_{2Q} \sin(2\Phi_Q)], \end{aligned} \quad (20)$$

where Q_l, Q_t are the longitudinal and transverse components of \vec{Q} , A_{1Q} and A_{2Q} are the coefficients of $\cos\phi$ and $(\cos\phi)^2$, and A_{0Q} is the term in (19) that is independent of ϕ . These are given in the Appendix, and Φ_Q , the upper limit on ϕ , is given by¹¹

$$\Phi_Q = \cos^{-1} \left(\frac{2k'_0 Q_0 - 2k'_l Q_l - m_L^2}{2k'_l Q_t} \right). \quad (21)$$

For the decay of a neutral heavy lepton into two charged leptons and a neutrino, as in (3) and (4), one may also be interested in the differential cross section of the other charged particle of three-momentum \vec{K} . This is the same in form as (20), that is,

$$\begin{aligned} \frac{d\sigma}{dq^2 dv dK_t^2 dK_l} &= \frac{G_1^2 G_2^2}{48(2\pi)^5 m_L \Gamma E^2 M K_0} \\ &\times [(A_{0K} + \frac{1}{2}A_{2K})\Phi_K + A_{1K} \sin\Phi_K \\ &+ \frac{1}{4}A_{2K} \sin(2\Phi_K)], \end{aligned} \quad (22)$$

where as before

$$\Phi_K = \cos^{-1} \left(\frac{2k'_0 K_0 - 2k'_l K_l - m_L^2}{2k'_l K_t} \right). \quad (23)$$

The coefficients A_{0K} , A_{1K} , and A_{2K} are also given in the Appendix.

E. Differential cross section neglecting polarization of L

The cross section $d\sigma_0$, neglecting polarization of the heavy lepton, is obtained by taking the product of $A_0\gamma_0$ instead of $\rho_0\mathfrak{D}_0$ from Eqs. (7) and (12) and is given by

$$\begin{aligned} \frac{d\sigma_0}{dq^2 dv dQ_t^2 dQ_l} &= \frac{G_1^2 G_2^2}{48(2\pi)^5 m_L \Gamma M E^2 Q_0} \\ &\times [(A_{00} + \frac{1}{2}A_{02})\Phi_Q + A_{01} \sin\Phi_Q \\ &+ \frac{1}{4}A_{02} \sin(2\Phi_Q)], \end{aligned} \quad (24)$$

where A_{00} , A_{01} , and A_{02} are given in the Appendix.

F. Differential cross section along the beam axis

Along the beam axis Q_t (or K_t) = 0 and Φ_Q (or Φ_K) = π ; and since $Q_0 = |Q_l|$, $K_0 = |K_l|$, the differential cross section (20) [and (22)] becomes a linear function of Q_l (or K_l) which can be analytically integrated to yield

$$\frac{d\sigma}{dq^2 dv dQ_t^2} \Big|_{Q_t=0} = C_-(1-g)^2 + C_+(1+g)^2, \quad (25)$$

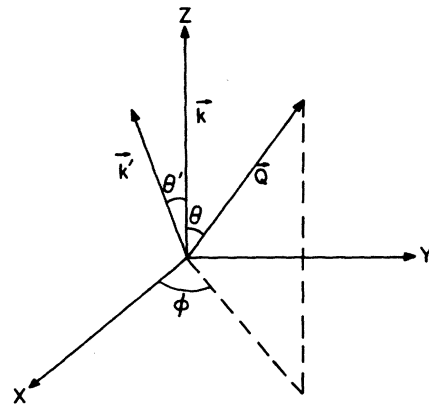


FIG. 2. The coordinate system used in the lab frame. The incident lepton with three-momentum \vec{k} is along the Z axis, the heavy lepton with momentum \vec{k}' makes an angle θ' with the Z axis and lies in the ZX plane. The outgoing charged lepton with momentum \vec{Q} is defined by the polar angles θ and the azimuthal angle ϕ .

where C_- and C_+ are given in the Appendix. On the other hand,

$$\left. \frac{d\sigma}{dq^2 dv dK_t^2} \right|_{K_t=0} = \frac{G_2^2 (1+g^2) m_L^3}{48\pi^3 \Gamma} \frac{d\sigma_p}{dq^2 dv}, \quad (26)$$

so that for both $V+A$ and $V-A$ couplings

$$\left. \frac{d\sigma}{dK_t^2} \right|_{K_t=0} = \frac{G_2^2 m_L^3}{24\pi^3} \frac{\sigma_p}{\Gamma}, \quad (27)$$

or, using (15), we get¹²

$$\left. \frac{d\sigma}{dK_t^2} \right|_{K_t=0} = \frac{8}{m_L^2} \sigma_p R, \quad (28)$$

where R is the branching ratio defined as

$$R = \frac{\Gamma_{L \rightarrow j}}{\Gamma}. \quad (29)$$

From (24) and the Appendix we also notice that only for $V-A$, i.e., for $g=1$,

$$\left. \frac{d\sigma}{dQ_t^2} \right|_{Q_t=0} \xrightarrow{g \rightarrow 1} \frac{8}{m_L^2} \sigma_p R. \quad (30)$$

Finally, from (24) we get

$$\left. \frac{d\sigma_0}{dQ_t^2} \right|_{Q_t=0} = \frac{[5(1+g^2) - 2g]}{m_L^2} \sigma_p R, \quad (31)$$

so that for $V-A$

$$\left. \frac{d\sigma_0}{dQ_t^2} \right|_{Q_t=0} \xrightarrow{g \rightarrow 1} \frac{8}{m_L^2} \sigma_p R, \quad (32)$$

and for $V+A$

$$\left. \frac{d\sigma_0}{dQ_t^2} \right|_{Q_t=0} \xrightarrow{g \rightarrow -1} \frac{12}{m_L^2} \sigma_p R. \quad (33)$$

III. NUMERICAL COMPUTATIONS

Numerical computations are done for $E=50$, 100, 200, and 500 GeV. The couplings G_1 and G_2 are taken identical to that for the muon. The branching ratio R into any one of the leptonic decay modes of L is taken to be¹³ 15%.

Introducing $\omega' = (2M\nu + M^2)/q^2$ the structure functions are parameterized as follows^{4,5}:

$$\begin{aligned} F_2(\omega') &= 1.1 \left[1 - \left(\frac{1}{\omega'} \right)^2 \right]^3, \\ F_1(\omega') &= \frac{1}{2} \omega' F_2(\omega'), \\ F_3(\omega') &= -|B| \omega' F_2(\omega'), \\ F_4(\omega') &= 0, \\ F_5(\omega') &= 2F_1(\omega'), \end{aligned} \quad (34)$$

where $F_1 = W_1$ and $F_i = (\nu/M)W_i$, with $i=2, 3, 4$, and 5. As indicated by the CERN Gargamelle data

on the $\bar{\nu}, \nu$ cross section ratio, we take $B=1$.⁵ The total cross section σ_p as a function of the heavy-lepton mass obtained by this parameterization is shown in Fig. 3 for $E=50, 100, 200$, and 500 GeV. We find that σ_p for $m_L = m_\mu$ in Fig. 3 compares very well with the experimental result

$$\sigma_p^\nu = (0.8 \pm 0.2) \times 10^{-38} E \text{ cm}^2. \quad (35)$$

Further, our parameterization (34) with $|B|=1$ also yields $\sigma_p(\bar{\nu})/\sigma_p(\nu) = \frac{1}{3}$ in agreement with the observed values.⁵

To obtain $d\sigma/dQ_t^2$, $d\sigma/dK_t^2$, and $d\sigma_0/dQ_t^2$, three-dimensional numerical integration of (20), (22), and (24) is done using the IBM systems 360, Scientific Subroutine Package, RANDU, for generating random numbers. 3×10^4 points are taken for each value of Q_t or K_t . Statistical fluctuations in the differential cross sections are estimated to be $\leq 2\%$.

IV. DISCUSSION OF RESULTS

To get a feeling for the cross section for production of heavy leptons we draw a graph for σ_p versus m_L (Fig. 3) for incident lepton energies of $E=50, 100, 200$, and 500 GeV in the lab frame. They exhibit a fast drop in the cross section with

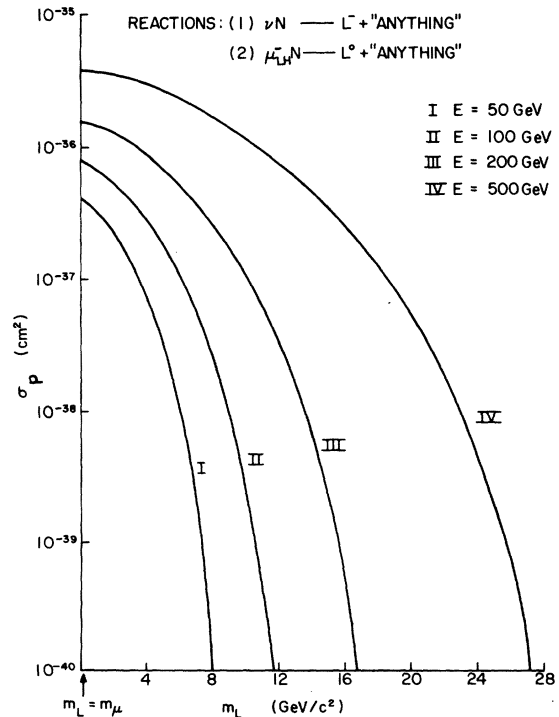


FIG. 3. The production cross section σ_p versus heavy-lepton mass m_L for incident energy $E=50, 100, 200$, and 500 GeV in the lab frame and assuming ($V-A$) coupling for L . Incident particle is ν or left-handed l^- .

an increase in m_L . For example, for $E = 100$ GeV, when the kinematical limit is $m_L \lesssim 13$ GeV, the cross section drops from 5.7×10^{-37} cm² for $m_L = 2$ GeV to 3.0×10^{-41} cm² for $m_L = 12$ GeV, a drop of ~ 4 orders of magnitude over a 10-GeV increase in mass.

The differential cross-section distribution with respect to (transverse momentum)², assuming (V-A) coupling for L , is shown in Figs. 4 and 5. In Figs. 4(a) and 4(b) the incident particle is ν or a left-handed μ^- and in Figs. 5(a) and 5(b) the incident particle is $\bar{\nu}$ or a right-handed μ^+ . These curves exhibit a very sharp drop with increase in transverse momentum. In fact, a numerical estimate of $\langle Q_t^2 \rangle$ shows that for $E = 100$ GeV and $m_L = 5$ GeV, $\langle Q_t^2 \rangle = 3.8$ GeV² when the kinematical limit is $Q_t^2 \lesssim 45$ GeV². The cross section $d\sigma/dQ_t^2$ again drops by 5 orders of magnitude over an increase of Q_t^2 from 0 to 35 GeV² for $E = 100$ GeV.

For (V-A) coupling of L , $d\sigma/dQ_t^2$ and $d\sigma/dK_t^2$ are identical as exhibited by (18).⁹ Again, it may be worth remembering that the branching ratio R throughout these computations has been taken to be 15%, and, in adapting these graphs to various models for heavy leptons, one must normalize them to the appropriate value of R given by the individual models.¹³

In Figs. 6(a) and 6(b) we redraw Figs. 4(a) and 4(b) by normalizing $d\sigma/dQ_t^2$ to $d\sigma/dQ_t^2|_{Q_t=0}$ using Eq. (30). We plot

$$P_{Q_t} = \left(\frac{d\sigma/dQ_t^2}{d\sigma/dQ_t^2|_{Q_t=0}} \times 100 \right) \%$$

versus Q_t^2 . These graphs are therefore independent of the branching ratio and hence can be directly compared to an experimental curve of (number of events with Q_t^2 /number of events with $Q_t=0$) versus Q_t^2 . In Fig. 6(a) we keep the energy

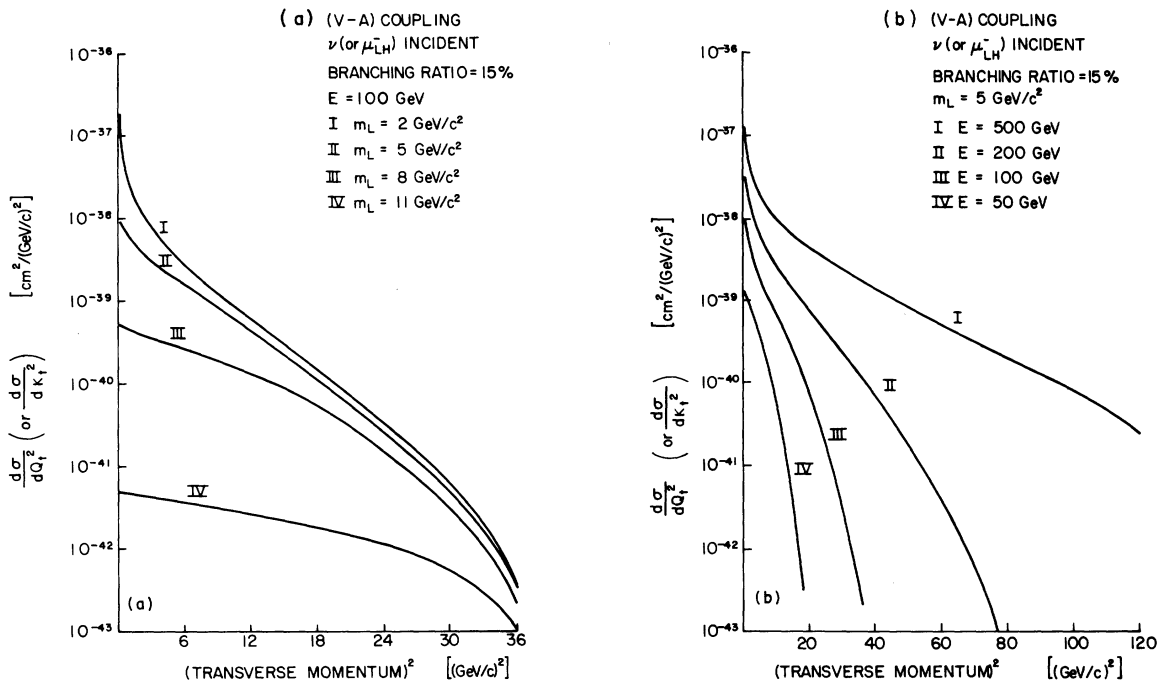


FIG. 4. In these graphs L is assumed to couple through (V-A) interaction. These curves apply to reactions of the type:

$$\nu(k) + N(p) \rightarrow L^-(k') + \text{"anything"}$$

$$\nu(k) + N(p) \rightarrow \nu(K) + l^-(Q) + \bar{\nu}_l(\bar{k})$$

and

$$l_{LH}^-(k) + N(p) \rightarrow L^0(k') + \text{"anything"}$$

$$l_{LH}^-(k) + N(p) \rightarrow l^-(K) + l'^+(Q) + \nu_{l'}$$

where l_{LH} is the left-handed electron or muon. For (V-A) coupling of L , $d\sigma/dQ_t^2 = d\sigma/dK_t^2$ as Eq. (18) reveals. In (a), we compare the distributions of the final charged lepton by keeping the energy of the incident lepton beam fixed at 100 GeV and taking the mass of the heavy lepton $m_L = 2, 5, 8$, and 11 GeV. In (b), m_L is held fixed and we take the incident lepton energy $E = 50, 100, 200$, and 500 GeV.

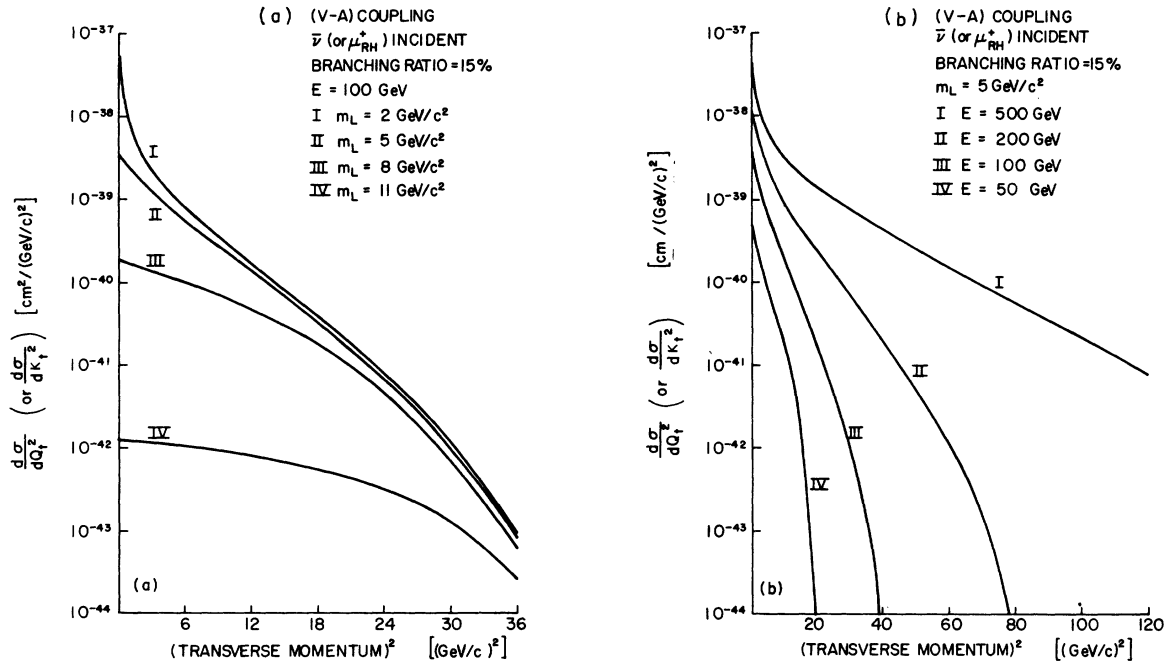
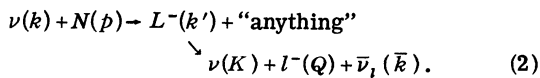


FIG. 5. Here the incident particle is taken to be $\bar{\nu}$ or l_{LH}^+ producing L^+ or \bar{L}^0 and decaying via $L^+ \rightarrow \bar{\nu}(K) + l^+(Q)$ or $\nu_i(\bar{k})$ or $\bar{L}^0 \rightarrow l^+(K) + l'^-(Q) + \bar{\nu}_i(\bar{k})$. Again $(V-A)$ coupling is assumed so that $d\sigma/dQ_t^2 = d\sigma/dK_t^2$.

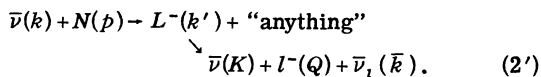
fixed at $E = 100$ GeV and vary the mass m_L from 2 to 11 GeV, and, in Fig. 6(b) we keep the mass fixed at 5 GeV and vary the energy from 50 to 500 GeV. Figure 6(a) exhibits a very strong dependence of P_{Q_t} on m_L whereas Fig. 6(b) shows practically no dependence of P_{Q_t} on E for the kinematically allowed values of Q_t^2 for each E .

If the $(V+A)$ coupling¹⁴ is instead assumed for L , then the differential cross section for incident right-handed ν or μ^- is shown in Fig. 7, and, for incident left-handed $\bar{\nu}$ or μ^+ the differential cross section is shown in Fig. 8. For $(V+A)$ coupling $d\sigma/dQ_t^2 \neq d\sigma/dK_t^2$ and we therefore draw both the distributions.

Throughout this work L^- is assumed to have the same lepton number as ν_i and l^- . So one has, for example,



If instead one is to assume that L^+ has the same lepton number as ν_i and l^- , as in certain gauge models, then the reaction producing the same charged final state as in (2) would be



It can be seen that the heavy-lepton current for reaction (2) is charge conjugate to the one in (2').

Hence, the case of $(V-A)$ coupling of L , i.e., $g=h=1$, for reaction (2) would correspond to $(V+A)$ current, i.e., $g=h=-1$, for reaction (2') and vice versa.

The effects due to polarization of the heavy lepton are shown in Fig. 9. The density matrix of the heavy lepton, expressed in Eqs. (7), (8), and (9), is very convenient for this purpose. The polarization vector S in the rest frame of L , given by

$$\hat{S} = \frac{\vec{B}_0}{A_0},$$

where B_0, A_0 are given in Eqs. (8) and (9), is used to obtain the degree of left-handedness P_{LH} of L , defined as

$$P_{\text{LH}} = [\frac{1}{2}(1 - \hat{S} \cdot \hat{k}') \times 100]\%. \quad (36)$$

Figure 9(a) shows P_{LH} as a function of the heavy-lepton energy k'_0 , keeping the scattering angle θ' fixed in the lab frame. The figure shows effects of changing the scattering angle θ' , which, incidentally, has to be very small because of the constraint $q^2 \leq 2M\nu$, the incident lepton energy E , and the mass m_L of the heavy lepton.

The consequence of all these dependences of \hat{S} on k'_0 , θ' , and E on the distributions of the emerging charged lepton is shown in Fig. 9(b). For this purpose we plot two functions D_0 and D_L , where

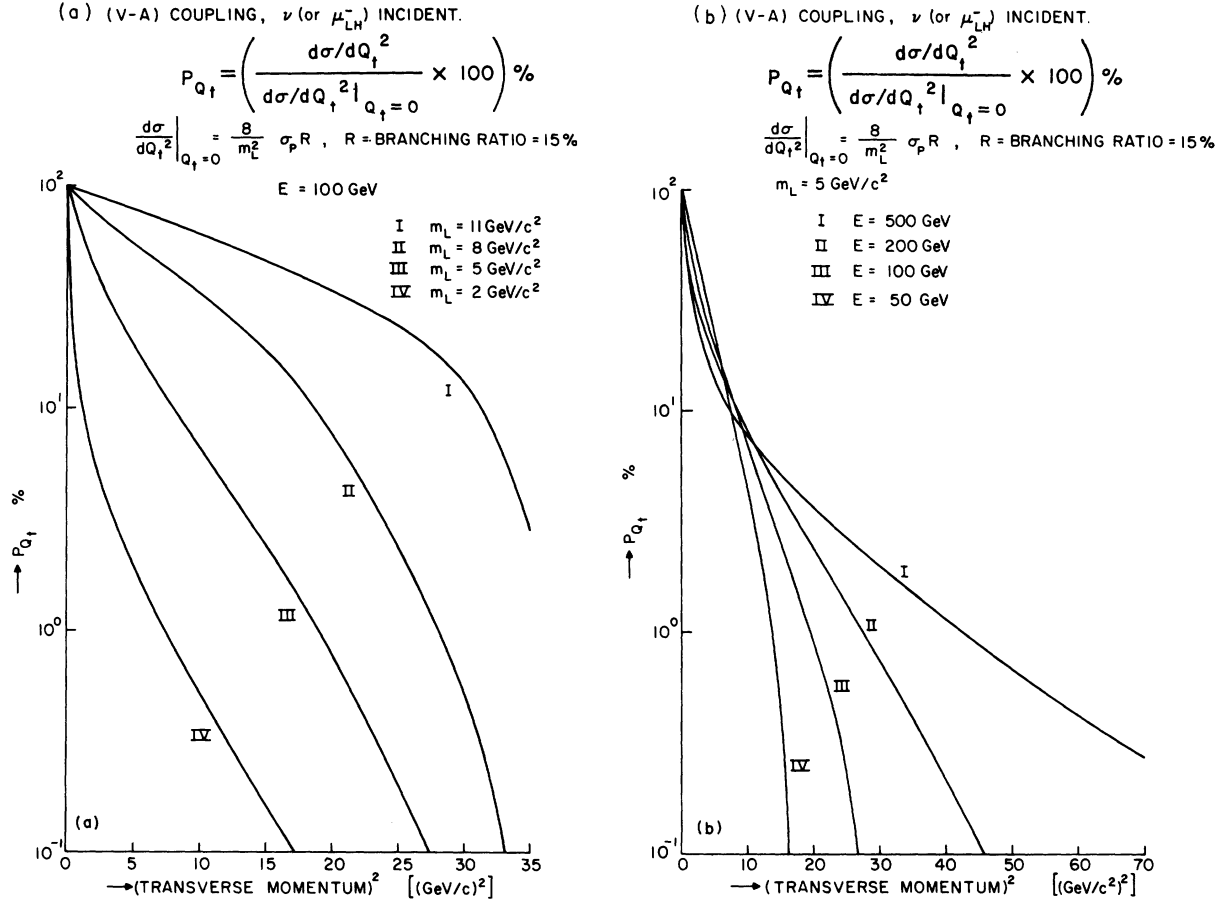


FIG. 6. This is the normalized version of Fig. 4. Since, for (V-A) coupling of L , $d\sigma/dQ_t^2 = (8/m_L^2)\sigma_p R$, such distributions are essentially normalized to the total cross section for a fixed value of m_L and are free of the value of R , unlike Fig. 4, and are, therefore, more readily comparable to an experimental graph of (number of events with $Q_t^2=0$) / (number of events with $Q_t^2=0$) versus Q_t^2 .

$$D_0 = \frac{d\sigma/dQ_t^2 - d\sigma_0/dQ_t^2}{d\sigma/dQ_t^2} \quad (37)$$

and

$$D_L = \frac{d\sigma/dQ_t^2 - d\sigma_L/dQ_t^2}{d\sigma/dQ_t^2} \quad (38)$$

Here $d\sigma/dQ_t^2$ is the distribution which incorporates all the polarization effects of the heavy lepton, $d\sigma_0/dQ_t^2$ is obtained by assuming the heavy lepton to be completely unpolarized and $d\sigma_L/dQ_t^2$ assuming the heavy lepton to be completely left-handed. In the region of experimental interest,² $Q_t \gtrsim 1.5 \text{ GeV}$, one finds that the polarization effects are rather significant.

ACKNOWLEDGMENT

I am deeply indebted to Professor Norman Christ for his sponsorship of this problem and for constant encouragement and advice in the course of this work.

APPENDIX

1. Coefficients A_{0Q} , A_{1Q} , and A_{2Q} of Eq. (20)

From (19),

$$I = \int \frac{d^3k'}{k'_0} \frac{d^3Q}{Q_0} F(k' \cdot Q) \theta(-(k' - Q)^2), \quad (A1)$$

where $F(k' \cdot Q)$ is a quadratic function of $(k' \cdot Q)$. Hence we may rewrite this as a quadratic function of $\cos \phi$. We write, for convenience,

$$F(k' \cdot Q) = B_Q - m_L^2 A_Q, \quad (A2)$$

where

$$B_Q = B_0 + B_1 \cos \phi + B_2 (\cos \phi)^2 \quad (A3)$$

and

$$A_Q = A_0 + A_1 \cos \phi, \quad (A4)$$

with

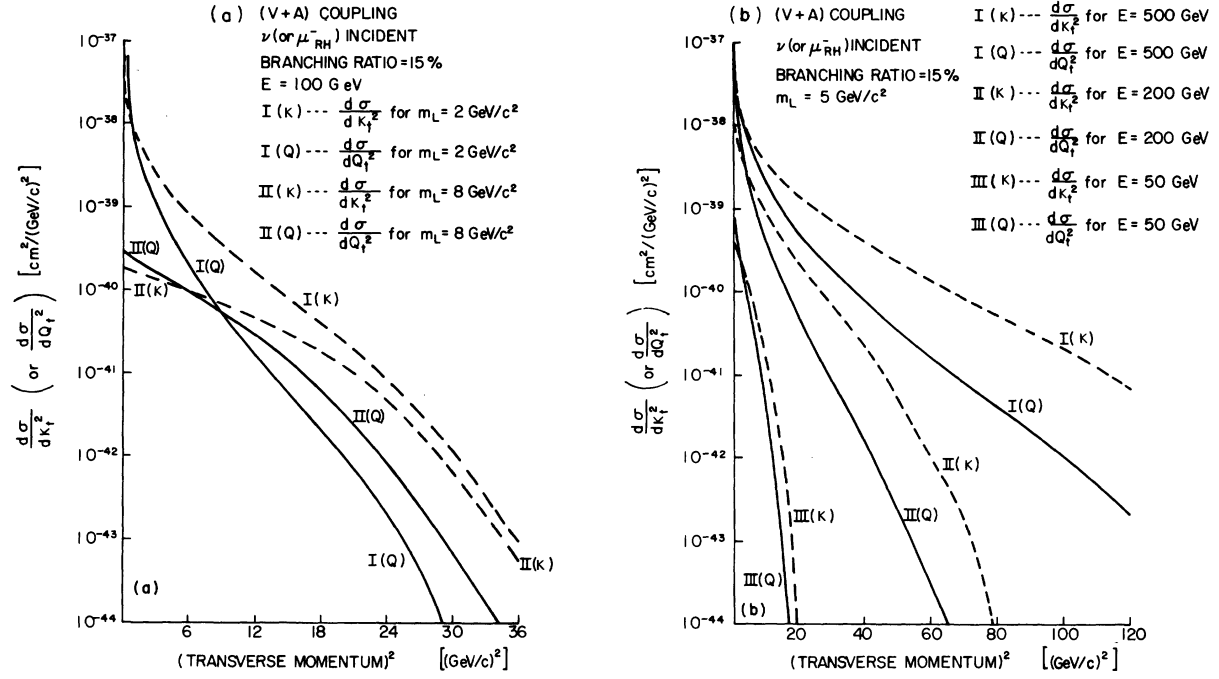


FIG. 7. Here (V+A) coupling for L is assumed, so the incident lepton is right-handed and $d\sigma/dQ_t^2 \neq d\sigma/dK_t^2$. The two charged leptons in the final state of decay of L^0 have significantly different distributions. In (a) we compare $d\sigma/dQ_t^2$ and $d\sigma/dK_t^2$ for fixed energy $E=100 \text{ GeV}$ and for $m_L=2$ and 8 GeV . In (b), we hold $m_L=5 \text{ GeV}$ fixed and compare $d\sigma/dQ_t^2$ and $d\sigma/dK_t^2$ for $E=50, 200, \text{ and } 500 \text{ GeV}$ (see Ref. 14).

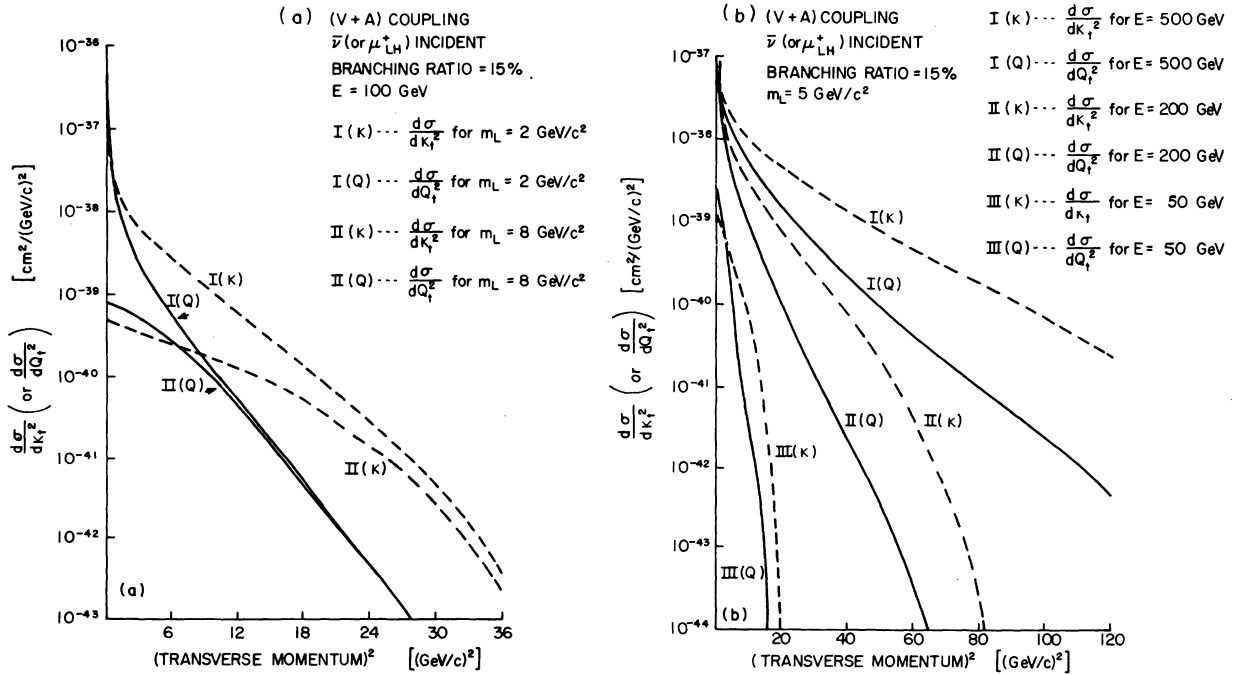


FIG. 8. These diagrams are for (V+A) coupling, assuming a left-handed incident antilepton. Again in (a), we compare $d\sigma/dQ_t^2$ and $d\sigma/dK_t^2$ for fixed E and for $m_L=2$ and 8 GeV . In (b), m_L is held fixed at 5 GeV and E is taken to be $50, 200, \text{ and } 500 \text{ GeV}$ (see Ref. 14).

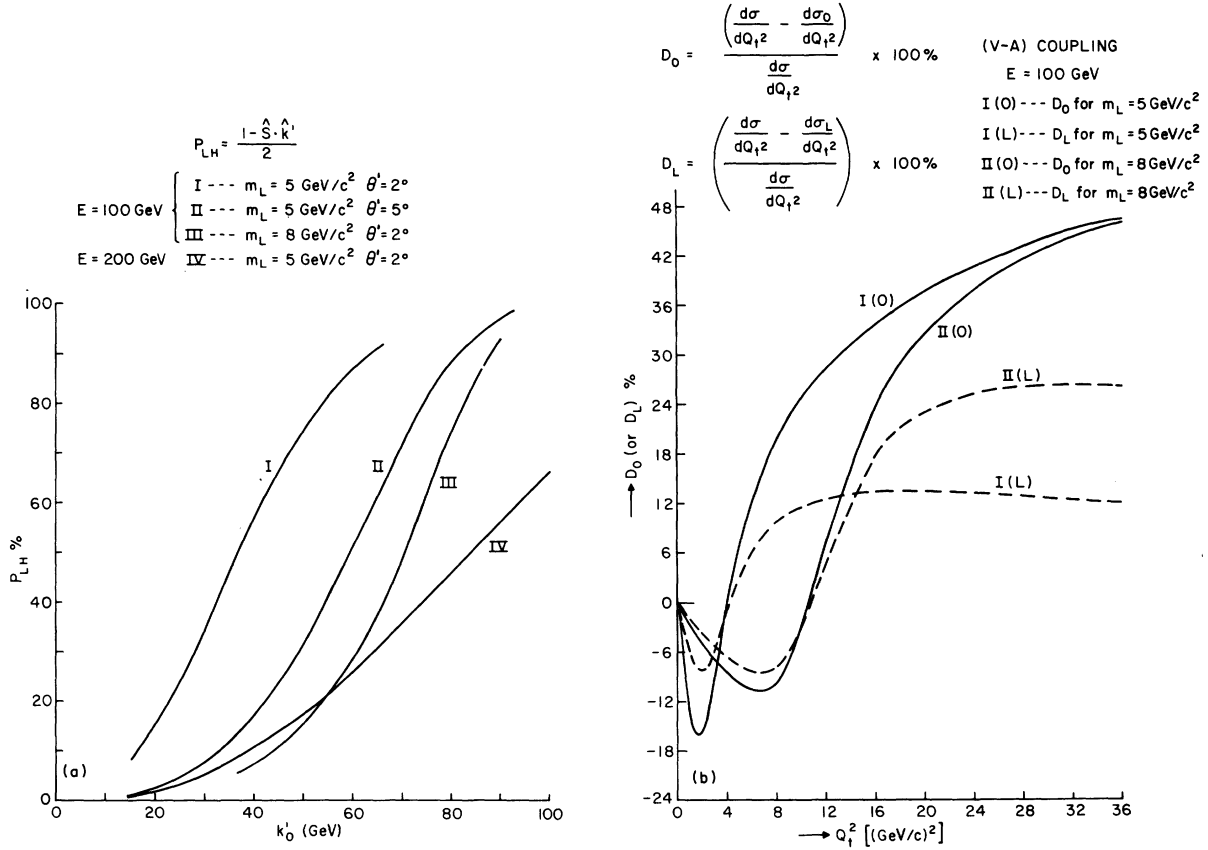
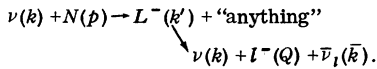


FIG. 9. These figures show the polarization effects of L in the reaction $\nu(k) + N(p)$



($V-A$) coupling for L is assumed. In (a), we plot the degree of left-handedness of L , defined by $P_{LH} = [\frac{1}{2}(1 - \hat{S} \cdot \hat{k}') \times 100]\%$, where \hat{S} is the polarization unit vector in the rest frame of L and \hat{k}' is the three-momentum unit vector of L in the lab frame, versus k'_0 which is the energy of the heavy lepton in the lab frame, keeping the scattering angle θ' fixed. The effects of the polarization of L on the spectrum of the final lepton under observation is shown in (b). The figure shows the corrections D_0 and D_L defined in Eqs. (37) and (38), as a function of the (transverse momentum)² for two different heavy-lepton masses $m_L = 5$ and 8 GeV with $E = 100 \text{ GeV}$.

$$B_0 = (k'_i Q_i - k'_0 Q_0) [C_0 + C_k k(Q_i - Q_0) - C_p M Q_0 + C_{k'} (k'_i Q_i - k'_0 Q_0)], \quad (A5)$$

$$B_1 = k'_i Q_i [C_0 + C_k k(Q_i - Q_0) - C_p M Q_0 + C_{k'} (k'_i Q_i - k'_0 Q_0)], \quad (A6)$$

$$B_2 = C_{k'} k_i'^2 Q_i^2, \quad (A7)$$

$$A_0 = k A_k (Q_i - Q_0) - A_p M Q_0 + A_{k'} (k'_i Q_i - k'_0 Q_0), \quad (A8)$$

and

$$A_1 = k'_i Q_i A_{k'}. \quad (A9)$$

The subscripts k , p , k' in the coefficients C 's and A 's imply that the latter are coefficients of $k \cdot Q$,

$p \cdot Q$, and $k' \cdot Q$, respectively, and subscript 0 denotes the term independent of Q in $F(k'Q)$.

The coefficients that appear in Eq. (20) are then given as

$$\begin{aligned} A_{0Q} &= B_0 - m_L^2 A_0, \\ A_{1Q} &= B_1 - m_L^2 A_1, \\ A_{2Q} &= B_2. \end{aligned} \quad (A10)$$

So we need to know C_0 , C_k , C_p , $C_{k'}$, and A_k , A_p , $A_{k'}$ of Eqs. (A5) to (A9) above. These are given below:

$$C_0 = -2(1+g)^2(1+h^2)m_L^2 C_{0i}, \quad (A11)$$

where

$$\begin{aligned}
C_{0t} &= 2W_1 k' \cdot k + \frac{W_2}{M^2} (k' \cdot k p^2 - 2k' \cdot p k \cdot p) \\
&\quad - \frac{W_3}{M^2} (k' \cdot p k \cdot q - k' \cdot q k \cdot p) \frac{2h}{1+h^2} \\
&\quad + \frac{W_4}{M^2} (k' \cdot k q^2 - 2k' \cdot q k \cdot q) \\
&\quad + \frac{W_5}{M^2} [(k' \cdot k p \cdot q - k' \cdot p k \cdot q - k' \cdot q k \cdot p)]; \quad (A12)
\end{aligned}$$

$$C_p = 8hm_L^2 [(1+g)^2 - 3(1-g)^2] C_{pt}, \quad (A13)$$

where

$$C_{pt} = 2 \frac{W_2}{M^2} k \cdot p + \frac{W_3}{M^2} \frac{1+h^2}{2h} k \cdot q + \frac{W_5}{M^2} k \cdot q; \quad (A14)$$

$$C_k = -8m_L^2 [(1+g)^2 - 3(1-g)^2] C_{kt}, \quad (A15)$$

where

$$\begin{aligned}
C_{kt} &= 2W_1 + \frac{W_2}{M^2} p^2 + \frac{W_3}{M^2} \frac{1+h^2}{2h} k \cdot p + \frac{W_4}{M^2} (q^2 - 2q \cdot k) \\
&\quad + \frac{W_5}{M^2} (q \cdot p - k \cdot p); \quad (A16)
\end{aligned}$$

$$\begin{aligned}
C_{k'} &= -4[3(1-g)^2(1-h)^2 + (1+g)^2(1+h)^2] C_{k't_1} \\
&\quad - 4[(1+g)^2(1+h)^2 - 3(1-g)^2(1-h)^2] C_{k't_2} \\
&\quad + 8hm_L^2 [3(1-g)^2 - (1+g)^2] C_{k't_3} \quad (A17)
\end{aligned}$$

where

$$C_{k't_1} = C_{0t} + \frac{W_3}{M^2} (k' \cdot p k \cdot q - k' \cdot q k \cdot p) \frac{2h}{1+h^2}, \quad (A18)$$

$$C_{k't_2} = \frac{W_3}{M^2} (k' \cdot q k \cdot p - k' \cdot p k \cdot q), \quad (A19)$$

$$C_{k't_3} = 2 \frac{W_4}{M^2} k \cdot q + \frac{W_5}{M^2} k \cdot p - \frac{W_3}{M^2} \frac{1+h^2}{2h} k \cdot p. \quad (A20)$$

Next,

$$A_k = 2hm_L^2 [(1+g)^2 - 6(1-g)^2] C_{kt}, \quad (A21)$$

$$A_p = -2hm_L^2 [(1+g)^2 - 6(1-g)^2] C_{pt}, \quad (A22)$$

and

$$\begin{aligned}
A_{k'} &= [6(1-g)^2(1-h)^2 + (1+g)^2(1+h)^2] C_{k't_1} \\
&\quad + [(1+h)^2(1+g)^2 - 6(1-g)^2(1-h)^2] C_{k't_2} \\
&\quad + 2hm_L^2 [(1+g)^2 - 6(1-g)^2] C_{k't_3}. \quad (A23)
\end{aligned}$$

2. Coefficients A_{0K} , A_{1K} , and A_{2K} of Eq. (22)

These are obtained in the same general way outlined in Appendix A 1.

$$\begin{aligned}
A_{0K} &= (k'_i K_i - k'_0 K_0) C_{0K} - (k'_i K_i - k'_0 K_0) B_k [2(k'_i K_i - k'_0 K_0) + m_L^2] + B_p MK_0 [2(k'_i K_i - k'_0 K_0) + m_L^2] \\
&\quad - EK_0 (\cos \theta' - 1) B_k [2(k'_i K_i - k'_0 K_0) + m_L^2], \quad (A24)
\end{aligned}$$

$$A_{1K} = 2k'_i K_i [C_{0K} - 4B_k (k'_i K_i - k'_0 K_0) + 2MK_0 B_p - 2B_k EK_0 (\cos \theta' - 1)] - m_L^2 B_k k'_i K_i, \quad (A25)$$

$$A_{2K} = -4k'_i{}^2 K_i^2 B_k. \quad (A26)$$

where C_{0K} , B_k , B_p , and B_k' are given below:

$$C_{0K} = -(1+h^2)m_L^2 [(1+g)^2 + (1-g)^2] C_{0t}, \quad (A27)$$

C_{0t} is given in Eq. (A12), and

$$B_k = 2h [(1+g)^2 - (1-g)^2] m_L^2 C_{kt}, \quad (A28)$$

$$B_p = -2h [(1+g)^2 - (1-g)^2] m_L^2 C_{pt}, \quad (A29)$$

$$\begin{aligned}
B_{k'} &= -[(1+g)^2(1+h)^2 + (1-g)^2(1-h)^2] C_{k't_1} \\
&\quad + [(1-g)^2(1-h)^2 - (1+g)^2(1+h)^2] C_{k't_2} \\
&\quad + 2hm_L^2 [(1-g)^2 - (1+g)^2] C_{k't_3}, \quad (A30)
\end{aligned}$$

where C_{kt} , C_{pt} , $C_{k't_1}$, and $C_{k't_3}$ are given in Appendix A 1.

3. A_{00} , A_{01} , and A_{02} of Eq. (24)

These are again obtained the same way as those in Appendix A 1:

$$\begin{aligned}
A_{00} &= -(1+h^2) C_{0t} (k'_i Q_i - k'_0 Q_0) \\
&\quad \times [9(1+g^2 - \frac{2}{3}g)m_L^2 \\
&\quad + 16(1+g^2 - g)(k'_i Q_i - k'_0 Q_0)], \quad (A31)
\end{aligned}$$

$$\begin{aligned}
A_{01} &= -(1+h^2) C_{0t} k'_i Q_i \\
&\quad \times [9(1+g^2 - \frac{2}{3}g)m_L^2 \\
&\quad + 32(1+g^2 - g)(k'_i Q_i - k'_0 Q_0)], \quad (A32)
\end{aligned}$$

$$A_{02} = -16(1+h^2) C_{0t} k'_i{}^2 Q_i^2 (1+g^2 - g), \quad (A33)$$

where C_{0t} is given in (A12).

4. C_+ , C_- occurring in Eq. (25)

$$C_+ = +2C(1+h^2)m_L^4 C_{0t}, \quad (A34)$$

where

$$C = \frac{G_1^2 G_2^2 \pi}{48(2\pi)^5 m_L \Gamma M E^2} \quad (A35)$$

and C_{0t} is given in (A12).

$$C_- = Cm_L^4 \left[-\frac{6km_L^2 h}{k'_0 + k'_L} C_{kt} + \frac{6hk'_0 m_L^2}{k'_t{}^2 + m_L^2} C_{pt} + 3(1-h)^2 (C_{k't_1} - C_{k't_2}) - 6m_L^2 h C_{k't_3} \right], \quad (\text{A36})$$

where C_{kt} , C_{pt} , $C_{k't_1}$, $C_{k't_2}$, and $C_{k't_3}$ are given in Eqs. (A16), (A14), (A18), (A19), and (A20).

*This research was supported in part by the U. S. Atomic Energy Commission.

¹Some of the more prominent papers on this topic are:

H. Georgi and S. L. Glashow, Phys. Rev. Lett. **28**, 1494 (1972); B. W. Lee, Phys. Rev. D **6**, 1188 (1972); J. Prentki and B. Zumino, Nucl. Phys. **B47**, 99 (1972). For a more complete list of references and a brief description of such theories, see J. D. Bjorken and C. H. Llewellyn Smith, Phys. Rev. D **7**, 887 (1973).

²R. Cester *et al.*, Princeton University report, 1973 (unpublished); W. Lee *et al.*, NAL Proposal No. 87, 1970 (unpublished); M. Bernadini *et al.*, paper submitted to the 6th International Symposium on Electron and Photon Interaction at High Energy, Bonn, Germany, August, 1973 (unpublished); B. C. Barish *et al.*, Caltech report, 1973 (unpublished).

³J. D. Bjorken and C. H. Llewellyn Smith, Phys. Rev. D **7**, 887 (1973).

⁴C. H. Albright, Phys. Rev. Lett. **28**, 1150 (1972).

⁵C. Baltay, invited paper at the Los Angeles meeting of the American Physical Society, December, 1972 (unpublished).

⁶Wherever in this paper the term "(V-A) coupling of the heavy lepton" is used, it means that in Eqs. (6) and (11) $h=g=+1$. Similarly, the term "(V+A) coupling of the heavy lepton" implies $h=g=-1$.

⁷We are assuming L^- to have the same lepton number as ν_l and l^- . If instead L^+ has the same lepton number as ν_l and l^- , as happens in certain gauge models, our graphs for (V-A) and (V+A) couplings of L , for the differential cross sections of the same outgoing charged lepton, will just get interchanged. [Also see Eqs. (2)

and (2').]

⁸We use $\vec{p} \cdot \vec{q} = \vec{p} \cdot \vec{q} - p_0 q_0$ and in our notation

$$\gamma_5 = \begin{pmatrix} 0 & -I \\ -I & 0 \end{pmatrix}.$$

⁹Note that we are assuming (V-A) coupling for the (e, ν_e) or (μ, ν_μ) currents even though L may couple either via (V-A) or (V+A) currents.

¹⁰We use the narrow-width approximation, that is,

$$\left| \frac{1}{k'^2 + m_L^2 - i m_L \Gamma} \right|^2 = \frac{\pi}{m_L \Gamma} \delta(k'^2 + m_L^2).$$

¹¹ Φ_Q is the upper limit on ϕ . This results from the constraint $(k' - Q)^2 \leq 0$.

¹²From (15),

$$\Gamma_{L \rightarrow l} = \frac{G_2^2 m_L^5}{4 \times 192 \pi^3} [(1+g)^2 + (1-g)^2].$$

¹³See Ref. 3. Assuming L^+ to have the same lepton number as ν_l and l^- they estimate $R(L_e^+ \rightarrow \mu^+ \nu_\mu \nu_e) \approx 15\%$ and $R(L_e^+ \rightarrow e^+ \nu_e \nu_e) \approx 30\%$, the difference coming from the identity of the two neutrinos in the final state of the second reaction. Throughout our numerical computations we are using $R=15\%$.

¹⁴For (V+A) coupling of the heavy lepton, i.e., $h=g=-1$, one needs right-handed incident leptons or left-handed incident antileptons for the production of such heavy leptons. In practice, right-handed ν or left-handed $\bar{\nu}$ are not available; hence the graphs for these cases are drawn here just for the sake of completion. (Also see Ref. 7.)